Organic & Biomolecular Chemistry

RSC Publishing

PAPER

View Article Online
View Journal | View Issue

Control of the ambident reactivity of the nitrite ion†

Cite this: *Org. Biomol. Chem.*, 2013, **11**, 648

Hai Dong,*[a,b] Martin Rahm,[b,c] Niranjan Thota,[b] Lingquan Deng,[b] Tore Brinck[b] and Olof Ramström*[b]

Received 7th June 2012,
Accepted 7th November 2012

DOI: 10.1039/c2ob26980e

www.rsc.org/obc

In previous studies, it was reported that a neighbouring equatorial ester group is essential for a good yield of nitrite-mediated triflate inversion, whereas with neighbouring benzyl ether groups or axial ester groups, mixtures are generally produced. In the present study, the origin of this difference was addressed. The ambident reactivity of the nitrite ion has been found to be the cause of the complex product formation observed, which can be controlled by a neighbouring equatorial ester group. Both N-attack and O-attack occur in the absence of the ester group, whereas O-attack is favoured in its presence. A neighbouring group assistance mechanism is proposed, in addition to steric effects, based on secondary interactions between the neighbouring ester group and the incoming nucleophile. High-level quantum mechanical calculations were carried out in order to delineate this effect. The theoretical results are in excellent agreement with experiments, and suggest a catalytic role for the neighbouring equatorial ester group.

Introduction

The ambident reactivity of nucleophiles and electrophiles is a general and long withstanding issue in chemistry, and its elusive nature is repeatedly addressed in modern selective synthesis.[1] Many intriguing examples involving ambident species have been reported, where reaction control presents continuous challenges. The ambident reactivity of the nitrite ion is one such example that has been discussed extensively, and the reactivity has been shown to depend on a variety of effects.[2] The Hard–Soft Acid–Base (HSAB) principle, and the perturbation molecular orbital (PMO) theory, have generally been applied in order to explain how nitrite- or nitro-products are generated, but a recent study from Mayr and co-workers conclude that the rationalization of ambident reactivity by the HSAB or the Klopman–Salem concept had to be abandoned.[1c] Instead, Marcus theory has been proposed to explain the reactivity patterns.[2b] As a consequence of the ambident nature, mixtures of nitro- and nitrite compounds are generally formed in the reactions.

The reactivity of the nitrite ion has been adopted in a highly useful transformation, the Lattrell–Dax reaction.[3] In the reaction, the anion is used as a reagent in epimerization reactions, where structures with inverse hydroxyl configuration can be produced under mild conditions. This substitution reaction proceeds through an unstable nitrite ester intermediate,[4] which is subsequently transformed into the *epi*-hydroxy structure. We found that a neighboring equatorial ester group plays a key role in the reaction, resulting in good inversion yields for a series of carbohydrate structures.[5] With benzyl ether groups or neighboring axial ester groups, on the other hand, mixtures are generally produced,[5,6] independent of the solvent polarity (DMF, MeCN, CH_2Cl_2, PhMe). Ring contraction and elimination products were often found in those complex mixtures.[7] Though these findings have been used to expand the utility of this highly useful reaction in carbohydrate synthesis,[8] the origin of the differences is still not clear. In the present study, this reaction has been used to delineate a neighbouring group assistance governing the outcome of the reaction. We report a new mechanism that is based on the nature of the neighboring groups, where different carbohydrate structures have been used as examples. The origin of this difference was addressed, and two hypotheses were challenged; firstly, the ambident reactivity of the nitrite ion is the cause of the complex product formation observed, and secondly, the *N*/*O* selectivity is controlled by the neighboring equatorial ester group.

[a]*Huazhong University of Science and Technology, School of Chemistry and Chemical Engineering, Luoyu Rd 1037, 430074 Wuhan, P. R. China. E-mail: hdong@mail.hust.edu.cn; Fax: (+86) 27-87793242*
[b]*Royal Institute of Technology (KTH), Department of Chemistry, Teknikringen 30, S-10044 Stockholm, Sweden. E-mail: ramstrom@kth.se; Fax: (+46) 8 7912333*
[c]*University of Southern California (USC), Loker Hydrocarbon Research Institute and Department of Chemistry, Los Angeles, CA 90089-1661, USA*

†Electronic supplementary information (ESI) available: ^{1}H and ^{13}C NMR spectra of compound **4**, **5** and **11**, IR spectra of compound **5** and **11**, ^{1}H and ^{1}H–^{1}H cosy spectra of triflate compounds, NMR analyse for inversion of compound **3**, **10** and **17**, Cartesian coordinates, energies and results of frequency calculations. See DOI: 10.1039/c2ob26980e

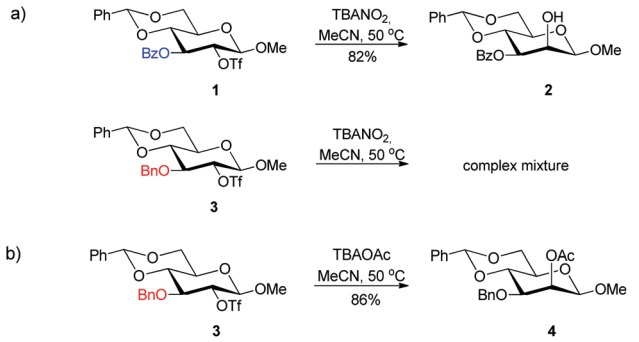

Scheme 1 (a) Examples of inversions with (a) nitrite; (b) acetate.

Results and discussion

In our previous studies, a series of triflates were tested as reactants in the substitution reactions with nitrite (Scheme 1a). For example, when compound **1** was allowed to react with nitrite in DMF or acetonitrile, the inversed compound **2** was isolated in 74% and 82% yield, respectively, whereas the analogous benzyl-protected compound **3** resulted in a complex mixture.[5] If this difference in product distribution is caused by the ambident nature of the nucleophile, results that are more independent of the neighboring group would be produced when non-ambident nucleophilic reagents are used. As can be seen, this was found to be the case, and good substitution yields were obtained for compound **3** when acetate was used as the nucleophile (Scheme 1b). This result supports the first hypothesis raised, pointing to the ambident nature of nitrite as the primary cause of mixture formation. Consequently, both the inversed nitro-product and nitrite-ester were formed by N/O-attack of nitrite for the epimerization of the substrates without a neighbouring equatorial ester group. Analogous reactions were also found in the ring opening of an epoxide by nitrite.[9] In all these cases, the nitro-products were highly acidic and might exist as the acinitronate, subsequently undergoing elimination of a beta-group to form more complicated contraction or fragmentation products at high temperature; whereas the nitrite esters are subsequently transformed into the hydroxyl groups with trace water. However, only O-attack of nitrite happened for the epimerization of the substrates with a neighbouring equatorial ester group, leading to exclusive products with an inversed hydroxyl group. Thus, the isolation of respective nitro-products from the mixtures will be a direct evidence for the ambident reactivity of nitrite in this Lattrell–Dax reaction.

The complex mixtures obtained were subsequently further analyzed (Scheme 2a). From compound **3**, three compounds could initially be identified after purification; compound **5** (50% yield), carrying a nitro-group in the equatorial position, and epimeric hydroxy-compounds **7** and **9**. Nitrite-ester **6** could be discriminated by ^{1}H NMR spectra combined with ^{1}H–^{1}H COSY (*cf.* ESI†). In a reference experiment using the *epi*-triflate analog of compound **3**, compounds **5** (41% yield) and **9** were again formed together with compound **8**. Further

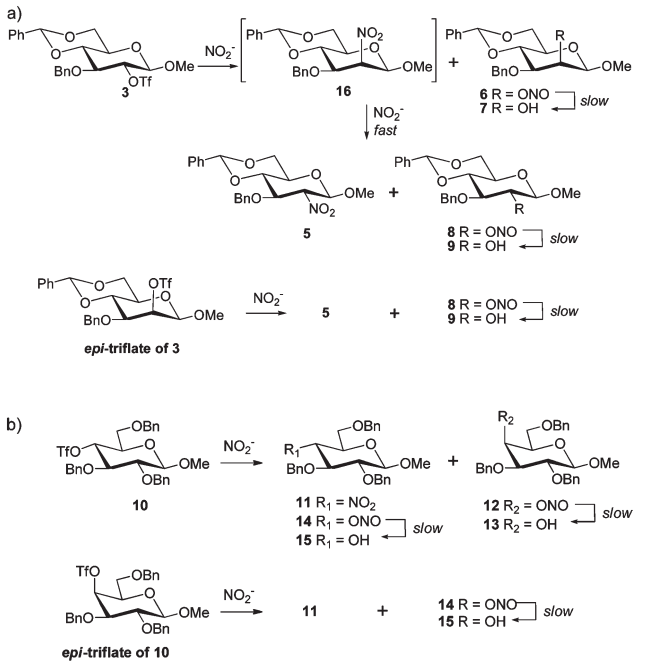

Scheme 2 (a) Identified compounds, proposed intermediate **16** and proposed pathway for product pattern resulting from compound **3**. (b) Identified compounds from reactions with **10**.

information could be obtained from ^{1}H NMR spectra of inversion with compound **3** (*cf.* ESI†), suggesting that an unknown compound and the compound **6** were formed immediately upon addition of nitrite to the solution. The nitrite-compound **6** was then slowly transformed into compound **7**, whereas the unknown compound relatively quickly reached a maximum level and gradually disappeared. Two new sets of signals were formed in the process; one of these was related to nitro-compound **5**, and the other to an unknown fragmentation compound. Very similar results were obtained when compound **10** was used in the reaction (Scheme 2b), where five different compounds could be identified (*cf.* ESI†). The unexpected compound **11**, carrying an equatorial nitro-group, was obtained in 18% yield. The *epi*-triflate analog of compound **10** was in this case also tested to corroborate the results, where compound **11**, was obtained in 36% yield.

Although not identified, the rapid initial formation of the unknown compound (**16**) must point to the axial nitro-compound resulting from N-attack at the triflate center. The unexpected nitro-compound then arose upon the gradual disappearance of the unknown compound. Deuterium exchange experiments involving compound **11** indicated no deprotonation under the conditions used. No exchange was thus observed with or without tetrabutylammonium nitrite at room temperature or even at 60 °C for 5 hours. The results suggest that compounds carrying a nitro group in the axial position are unstable and lead to the more stable structures with the substituents in the equatorial position. Though the deuterium exchange experiments gave no direct evidence, a reasonable mechanism for the conversion should involve

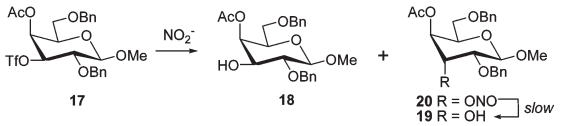

Scheme 3 Identified compounds and proposed mechanism for nitrite-mediated epimerization of compound **17**.

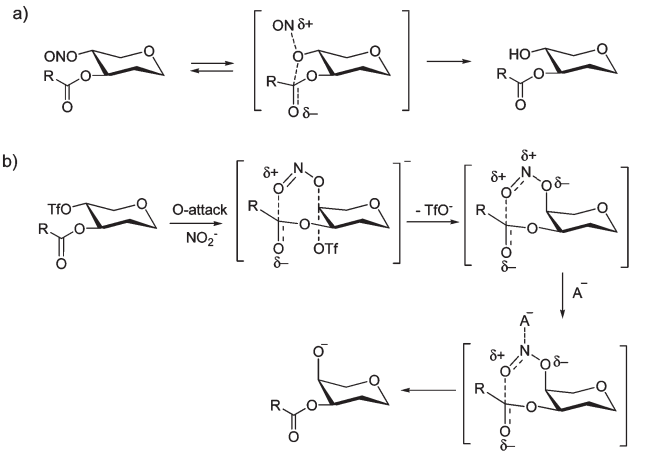

Scheme 4 (a) Suggested intramolecular leaving group assistance according to Thatcher; (b) suggested neighboring group assistance by us.

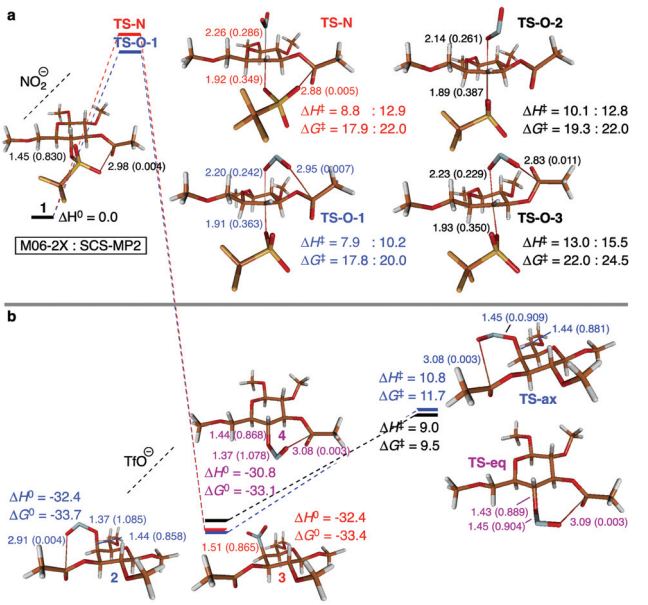

Fig. 1 (a) Nitrite insertion: oxygen-attack (blue) is assisted by a favorable interaction between the nitrite anion and the neighboring equatorial ester group. This type of interaction is not possible in the case of nitrogen-attack (red) and is a likely explanation for the kinetic control of the epimerization reaction. (b) Hydrolysis proceeds rapidly by initial elimination of NO radicals. DFT-M06-2X and SCS-MP2 energies are reported in kcal mol^{-1} and bond lengths in Ångström (Å). Wiberg bond indices are given within parenthesis.

deprotonation and reprotonation at the carbon with nitrate. The overall process for compound **3** is outlined in Scheme 2a.

The reaction between nitrite and compound **17**, carrying a neighboring ester group in the axial position, was also analyzed (*cf.* Scheme 3). When this reaction was carried out in DMF at 50 °C, a very complex mixture was produced that was difficult to analyze. For this reason, the reaction was instead analyzed in acetonitrile at room temperature. The reaction proved in this case very sluggish but column chromatography and ^{1}H NMR could be used to identify the main species formed. Hydroxy compound **19** was isolated from this reaction as a major component, together with lower amounts of its *epi*-hydroxy analog **18**. No major formation of nitro-compounds was in this case seen. In analogy to the results for compounds **3** and **10**, the axial nitro group would also be unstable, leading to the more stable equatorial species. In contrast to these results, when compound **17** was instead tested in *d*-benzene, compound **19**, and its nitrite precursor **20** were the major products due to supramolecular control.[8f] All these results support the first hypothesis raised, that the ambident nature of the nitrite ion is a major cause for the complex mixture formation.

Furthermore, during the nitrite-mediated inversion of triflate structures with a neighboring equatorial ester group, neither nitro products nor nitrite products were observed when the same reactions were performed. Instead, the inversed hydroxyl group products were always formed in near quantitative yields. These results indicate that only O-attack occurred, and the intermediate nitrite products were instantly transformed to their hydroxy analogs, due to the effect of the neighboring ester group. The origin of this phenomenon points to the occurrence of secondary interactions between the nitrite nucleophile, and the nitrite ester, with the neighboring ester functionality. As well kinetic effects, statistic effects and steric reasons play roles in the reaction; but considering the same pattern for many different structures, these effects are unlikely to be inclusive.

The hydrolysis of alkyl nitrites has been studied and the mechanism was suggested to be concerted.[4a,10] The acid-catalyzed hydrolysis of alkyl nitrites is quite fast, whereas the basic hydrolysis of alkyl nitrites is an extremely slow process, owing to the higher electronegativity of nitrogen, and the presence of a lone pair, compared to the hydrolysis of esters. Furthermore, an explanation for the rapid transformation of the nitrite intermediates has been proposed by Thatcher and co-workers.[11] During the hydrolysis of nitrite esters, intramolecular Lewis acid or charge transfer catalysis by the β-nitrate group was proposed, in which the β-nitrate substituent assists the departure of the leaving group. The mechanism was supported by *ab initio* and semi-empirical molecular orbital calculations. In the present case, the analogous five-membered ring mechanism is plausible, where the ester group assists the departure of the leaving group (Scheme 4a). However, according to our further quantum chemical study, a seven-membered ring mechanism seems more reasonable (Scheme 4b).

It is more difficult to explain how the neighboring equatorial ester group can restrain the occurrence of an N-attack or promote the O-attack pathway. A plausible mechanism involves

secondary interactions between the incoming nitrite and the neighboring ester group, guiding the reaction towards O-attack (Scheme 4b), subsequently followed by assisted hydrolysis of nitrite ester. For this reason, quantum mechanical calculations were carried out in order to delineate this effect (Fig. 1). The inversion of the 4-*O*-substituent of a 3-*O*-acetylated glucoside derivative in acetonitrile was evaluated, where the 2 and 6-hydroxyl groups were methylated. Structure optimization and frequency analyses were performed using the recent hybrid meta exchange-correlation density functional M06-2X[12] in Gaussian 09,[13] using a 6-31+G(d,p) basis set, together with an implicit treatment of acetonitrile solvent through the SCRF/PCM approximation. M06-2X includes long-range dispersion effects through empirical means and has been shown highly reliable for calculating main group thermochemistry.[12,14] Final single-point energies in solution were obtained at the M06-2X/cc-pVTZ level using Gaussian 09. Solution energies were also evaluated with the Conductor-like Screening Model (COSMO)[15] and spin component scaled second-order Møller–Plesset perturbation theory, at the SCS-MP2/cc-pVDZ[16] level, as implemented in the ORCA 2.9 code.[15] The MP2 method includes *ab initio* approximations to all relevant long-range interactions, *i.e.* electrostatics, dispersion and induction, and the SCS-approach has been shown to improve the accuracy of MP2 considerably.[16] Wiberg bond indices were calculated from natural atomic orbitals (NAOs) obtained from the M062X/cc-pVTZ wave functions.

The rate difference between two competing reaction barriers can be estimated using Boltzmann statistics and transition state theory (TST). As a reference it can be mentioned that a selectivity of 98% corresponds to a barrier difference of only 2.3 kcal mol^{-1} at 20 °C. Such a difference is close to the accuracy of even the most advanced quantum mechanical treatments available for this size of system. The energy of five conformers of **1** were initially evaluated at the B3LYP/6-31+G(d,p) level. The lowest one was selected for further mechanistic studies using PCM-M06-2X and COSMO-SCS-MP2 calculations. Whereas only one transition state for nitrogen attack was found (*cf.* **TS-N** in Fig. 1a), three energetically reasonable ($\Delta G^{\ddagger}$ < 25 kcal mol^{-1}) transition states for oxygen attack were identified (*cf.* **TS-O-1**, **TS-O-2** and **TS-O-3** in Fig. 1a), with **TS-O-1** being the lowest at all levels of theory. The accurate M06-2X DFT functional provided an activation enthalpy barrier for nitrite–oxygen attack (**TS-O-1**) that is 0.9 kcal mol^{-1} lower than the corresponding nitrogen attack (**TS-N**). The same difference is 2.7 kcal using the SCS-MP2 method, also in favour of **TS-O-1**. These values are closely mirrored in the thermally uncorrected SCF energies (0.5 and 2.4 kcal mol^{-1}, respectively). The free Gibbs energy barriers (at 20 °C and 1 M) are in good agreement with reactions that proceed readily at ambient conditions ($\Delta G^{\ddagger}$ = 18–22 kcal mol^{-1}, Fig. 1a). The $\Delta G^{\ddagger}$ values also predict a kinetic prevalence for oxygen-attack, at both levels of theory.

Wiberg bond indices are calculated from the overlap of NAOs residing on neighbouring atoms, and are facile measures of covalent interaction. However, such indices are by construction poor measures of interactions dominated by van der Waals dispersion, and should not be interpreted as such. Calculated bond lengths together with Wiberg bond order analyses show **TS-O-1** to be a slightly earlier transition state than **TS-N** (Fig. 1). In **TS-N** the triflate and ester groups maintain orientations similar to those in the ground state **1**, with one oxygen of the triflate coordinated towards the partially positive carbonyl carbon of the ester group. Interestingly, in **TS-O-1**, the ester group is twisted by 50° and the triflate–carbonyl interaction is broken in favour of a nitrite–carbonyl interaction. This interaction is not possible in the case of nitrite–nitrogen attack. A similar twist is also observed in **TS-O-2**. However, in this case the ester group is in lessened proximity to the nitrite anion. The noticeable twist of the ester group, which later is present in both reaction products, enables long-range attractive interactions between the face of the ester and the approaching nitrite anion in the case of **TS-O-1**. A rough estimate of this interaction can be obtained by comparing **TS-O-1** with **TS-O-2**, which are close to identical geometrically except for the orientation of the nitrite anion. Positioning of the nitrite anion adjacent to the equatorial ester group reduces the energy by 2 kcal mol^{-1}. These results are in excellent agreement with experiment, and suggest a catalytic role for the ester group that would explain the dependence of the *N*/*O*-selectivity to the group's placement on the carbohydrate backbone.

Fig. 1b depicts processes by which rapid hydrolysis of the intermediate **2**, or its equatorial isomer **4**, can occur by elimination of NO radicals through **TS-ax** and **TS-eq**, respectively. These processes are likely also affected by interactions with the equatorial ester group to some extent. However, as these reactions are not rate determining for the over-all process such interactions are of no consequence for the obtained product mixture. More exact details of the hydrolysis mechanism are likely indeterminate without explicit consideration of neighbouring water molecules and solvent interactions. Consequently, we can conclude that hydrolysis proceeds with reaction barriers equal to or lower than ~12 kcal mol^{-1}.

These results point to the requirement of an equatorial ester group for good inversion yields. Leaving group assistance has been proposed, and a secondary interaction exerted by the equatorial ester group has also been demonstrated in complement to steric effects. The second hypothesis raised is thus supported, and the *N*/*O* selectivity is in all probability dependent on the neighboring group pattern.

Conclusions

The ambident reactivity of the nitrite anion in Lattrell–Dax-type epimerization reactions has been studied. It was found that both N- and O-attack occur in the absence of a neighboring equatorial ester group, whereas the N-attack is excluded in its presence. A neighbouring group assistance mechanism has been proposed, in addition to steric and kinetic effects, based on secondary interactions with the neighboring equatorial

ester group and the incoming nucleophile. From these results, we have shown that the Lattrell–Dax reaction can be well incorporated into synthesis, generating various target structures in a controllable way.

Experimental section

General

All commercially available starting materials and solvents were of reagent grade and dried prior to use. Chemical reactions were monitored with thin-layer chromatography using precoated silica gel 60 (0.25 mm thickness) plates. Flash column chromatography was performed on silica gel 60 (0.040–0.063 mm). Optical rotations were measured at the sodium D line at ambient temperature. ^{1}H and ^{13}C spectra were recorded with a 400 MHz or 500 MHz instrument at 298 K in $CDCl_3$ and CD_3CN, using the residual signals from $CHCl_3$ (^{1}H: δ = 7.26 ppm; ^{13}C: δ = 77.2 ppm) and CHD_2CN (^{1}H: δ = 1.94 ppm; ^{13}C: δ = 118.3 ppm) as internal standard. ^{1}H peak assignments were made by first order analysis of the spectra, supported by standard ^{1}H–^{1}H correlation spectroscopy (COSY). IR spectra were recorded from 400 to 4000 cm^{-1} at ambient temperature.

General synthesis of triflate derivatives

To a solution of the suitably *O*-protected methyl β-D-glycoside, carrying an unprotected OH at C2, C3 or C4 (0.94 mmol), in CH_2Cl_2 (5 mL) was added pyridine (0.65 mL) at −20 °C. Trifluoromethanesulfonic anhydride (0.53 g, 1.88 mol) in CH_2Cl_2 (2 mL) was added dropwise, and the mixture was stirred while allowing to warm from −20 °C to 10 °C over 2 h. The resulting mixture was subsequently diluted with CH_2Cl_2 and washed with 1 M HCl, aqueous $NaHCO_3$, water, and brine. The organic phase was dried with $MgSO_4$ and concentrated *in vacuo* at low temperature. The residue could be identified by ^{1}H NMR in quantitative yield and was used directly in the next step or in further ^{1}H NMR-experiments without further purification.

General inversion of triflate derivatives

$TBANO_2$ (5 equiv.) was added to a solution of the protected triflate residue (200 mg) in solvents (DMF, MeCN, CH_2Cl_2, PhMe) (2.0 mL). After stirring at 20 °C–50 °C for 1–6 h, the mixture was diluted with CH_2Cl_2 and washed with brine. The organic phase was dried with $MgSO_4$ and concentrated *in vacuo*. Purification of the residue by flash column chromatography (3 : 1 to 1 : 1 hexane–ethyl acetate) afforded the inversion products.

General inversion of triflate derivatives in *d*-solvents

$TBANO_2$ (5 equiv.) was added to a solution of the purified triflate residue (5 mg) in *d*-solvents (MeCN, benzene) (0.5 mL). The reaction was performed in NMR-tube at room temperature for 0–48 h. ^{1}H NMR spectra were recorded with a Bruker Avance 400 instrument or Bruker DMX 500 instrument at 298 K, using the residual signals from *d*-acetonitrile and *d*-benzene as internal standard.

Methyl 2-*O*-acetyl-3-*O*-benzyl-4,6-*O*-benzylidene-β-D-mannoside (4). ^{1}H NMR ($CDCl_3$, 400 MHz): δ 7.24–7.54 (m, 10 H, 2 × Bn), 5.65 (d, 1 H, $J_{2,3}$ 3.0 Hz, H_2), 5.62 (s, 1 H, $O_2CHC_6H_5$), 4.75, 4.64 (d, 2 H, $J_{a,b}$ 12.1 Hz, $OCH_aH_bC_6H_5$), 4.51 (s, 1 H, H_1), 4.35 (dd, 1 H, $J_{6a,6b}$ 10.3 Hz, $J_{6a,5}$ 4.9 Hz, H_{6a}), 4.03 (t, 1 H, $J_{4,3}$, $J_{4,5}$ 9.7 Hz, H_4), 3.91 (t, 1H, $J_{6b,5}$, $J_{6b,6a}$ 10.3 Hz, H_{6b}), 3.73 (dd, 1 H, $J_{3,2}$ 3.0 Hz, $J_{3,4}$ 9.7 Hz, H_3), 3.53 (s, 3 H, OMe), 3.34–3.44 (m, 1 H, H_5), 2.21 (s, 3 H, OAc); ^{13}C NMR ($CDCl_3$, 125 MHz): δ 170.6, 137.8, 137.5, 129.1, 128.6, 128.4, 127.9, 127.8, 126.2, 101.7, 100.9, 78.1, 75.7, 71.9, 68.9, 68.6, 67.4, 57.7; $[\alpha]_D^{20}$ = −71 (c = 0.7, $CHCl_3$); HRMS: calcd For $C_{23}H_{26}O_7$ [M + Na^+]: 437.1576. Observed: 437.1594.

Methyl 3-*O*-benzyl-4,6-*O*-benzylidene-2-deoxy-2-nitro-β-D-glucoside (5). ^{1}H NMR (CD_3CN, 500 MHz): δ 7.24–7.54 (m, 10 H, 2 × Bn), 5.68 (s, 1 H, $O_2CHC_6H_5$), 4.90 (d, 1 H, $J_{1,2}$ 8.1 Hz, H_1), 4.84, 4.60 (d, 2 H, $J_{a,b}$ 11.3 Hz, $OCH_aH_bC_6H_5$), 4.57 (dd, 1 H, $J_{2,1}$ 8.1 Hz, $J_{2,3}$ 10.1 Hz, H_2), 4.36 (dd, 1 H, $J_{3,2}$ 10.1 Hz, $J_{3,4}$ 9.4 Hz, H_3), 4.32 (dd, 1 H, $J_{6a,6b}$ 10.3 Hz, $J_{6a,5}$ 4.9 Hz, H_{6a}), 3.83 (t, 1 H, $J_{4,3}$, $J_{4,5}$ 9.4 Hz, H_4), 3.82 (t, 1H, $J_{6b,5}$, $J_{6b,6a}$, 10.2 Hz, H_{6b}), 3.60–3.68 (m, 1 H, H_5), 3.47 (s, 3 H, OMe.); ^{13}C NMR (CD_3CN, 125 MHz): δ 138.6, 138.5, 130.0, 129.3, 129.2, 129.0, 128.9, 127.1, 102.1, 101.8, 90.7, 81.8, 78.3, 75.0, 68.8, 67.1, 57.9; FTIR (KBr, cm^{-1}): strong absorption at 1550 and 1365 cm^{-1}; $[\alpha]_D^{20}$ = −16 (c = 0.3, $CHCl_3$); HRMS: calcd For $C_{21}H_{23}NO_7$ [M + Na^+]: 424.1372. Observed: 424.1370.

Methyl 2,3,6-tri-*O*-benzyl-4-deoxy-4-nitro-β-D-glucoside (11). ^{1}H NMR (CD_3CN, 400 MHz): δ 7.16–7.37 (m, 15 H, 3 × Bn), 4.92, 4.70 (d, 2 H, $J_{a,b}$ 11.9 Hz, $OCH_aH_bC_6H_5$), 4.82, 4.53 (d, 2 H, $J_{c,d}$ 10.8 Hz, $OCH_cH_dC_6H_5$), 4.72 (t, 1 H, $J_{4,3}$, $J_{4,5}$ 10.3 Hz, H_4), 4.84, 4.60 (d, 2 H, $J_{e,f}$ 11.3 Hz, $OCH_eH_fC_6H_5$), 4.41 (d, 1 H, $J_{1,2}$ 7.8 Hz, H_1), 4.23 (dd, 1 H, $J_{3,2}$ 9.1 Hz, $J_{3,4}$ 10.3 Hz, H_3), 3.93–3.99 (m, 1 H, H_5), 3.65 (dd, 1 H, $J_{6a,6b}$ 10.8 Hz, $J_{6a,5}$ 3.5 Hz, H_{6a}), 3.58 (s, 3 H, OMe), 3.56 (dd, 1H, $J_{6b,6a}$ 10.8 Hz, $J_{6b,5}$ 4.0 Hz, H_{6b}), 3.46 (dd, 1 H, $J_{2,1}$, 7.8 Hz, $J_{2,3}$ 9.1 Hz, H_2); ^{13}C NMR ($CDCl_3$, 125 MHz): δ 138.1, 137.5, 137.4, 128.7, 128.6, 128.5, 128.2, 128.1, 128.0, 127.9, 104.9, 87.1, 81.8, 80.4, 75.9, 75.0, 74.0, 72.5, 68.9, 57.5; FTIR (KBr, cm^{-1}): strong absorption at 1550 and 1365 cm^{-1}; $[\alpha]_D^{20}$ = −10 (c = 0.7, $CHCl_3$); HRMS: calcd For $C_{28}H_{31}NO_7$ [M + Na^+]: 516.1998. Observed: 516.2008.

Acknowledgements

This work was supported by the Fundamental Research Funds for the Central Universities (HUST: 2012QN146), the National Nature Science Foundation of China (Nos. 21272083), the Chutian Project-Sponsored by Hubei Province, the Swedish Research Council and the Royal Institute of Technology.

Notes and references

1 (*a*) T. A. Nigst, J. Ammer and H. Mayr, *Angew. Chem., Int. Ed.*, 2012, **51**, 1353; (*b*) N. Vujkovic, V. Cesar, N. Lugan and G. Lavigne, *Chem.–Eur. J.*, 2011, **17**, 13151; (*c*) H. Mayr, M. Breugst and A. R. Ofial, *Angew. Chem., Int. Ed.*, 2011, **50**,

6470; (*d*) F. Blanco, I. Alkorta, I. Rozas, M. Solimannejad and J. Elguero, *Phys. Chem. Chem. Phys.*, 2011, **13**, 674; (*e*) R. Dobrovetsky, L. Zborovsky, D. Sheberla, M. Botoshansky, D. Bravo-Zhivotovskii and Y. Apeloig, *Angew. Chem., Int. Ed.*, 2010, **49**, 4084.

2 (*a*) M. Baidya, S. Kobayashi and H. Mayr, *J. Am. Chem. Soc.*, 2010, **132**, 4796; (*b*) M. Breugst, H. Zipse, J. P. Guthrie and H. Mayr, *Angew. Chem., Int. Ed.*, 2010, **49**, 5165; (*c*) J. S. M. Anderson and P. W. Ayers, *Phys. Chem. Chem. Phys.*, 2007, **9**, 2371; (*d*) T. J. Broxton, D. M. Muir and A. J. Parker, *J. Org. Chem.*, 1975, **40**, 3230; (*e*) R. G. Pearson and J. Songstad, *J. Am. Chem. Soc.*, 1967, **89**, 1827–1836.

3 (*a*) R. Lattrell and G. Lohaus, *Justus Liebigs Ann. Chem.*, 1974, 901; (*b*) R. Albert, K. Dax, R. W. Link and A. E. Stutz, *Carbohydr. Res.*, 1983, **118**, C5.

4 (*a*) E. Iglesias, L. Garciario, J. R. Leis, M. E. Pena and D. H. L. Williams, *J. Chem. Soc., Perkin Trans. 2*, 1992, 1673; (*b*) E. Iglesias and A. Fernandez, *J. Chem. Soc., Perkin Trans. 2*, 1998, 1691.

5 H. Dong, Z. Pei and O. Ramström, *J. Org. Chem.*, 2006, **71**, 3306.

6 (*a*) R. W. Binkley, *J. Org. Chem.*, 1991, **56**, 3892; (*b*) R. W. Binkley, *J. Carbohydr. Chem.*, 1994, **13**, 111; (*c*) A. Liakatos, M. J. Kiefel and M. von Itzstein, *Org. Lett.*, 2003, **5**, 4365.

7 (*a*) M. Kassou and S. Castillon, *J. Org. Chem.*, 1995, **60**, 4353; (*b*) A. EI Nemr and T. Tsuchiya, *Carbohydr. Res.*, 1997, **303**, 267.

8 (*a*) J. Karban, I. Cisarova, H. F. Schaller, L. C. Stastna and J. Sykora, *Org. Biomol. Chem.*, 2012, **10**, 394; (*b*) Y. M. Lee, D. J. Baek, S. Lee, D. Kim and S. Kim, *J. Org. Chem.*, 2011, **76**, 408; (*c*) W. W. Li, T. D. W. Claridge, Q. H. Li, M. R. Wormald, B. G. Davis and H. Bayley, *J. Am. Chem. Soc.*, 2011, **133**, 1987; (*d*) J. Karban, J. Sykora, J. Kroutil, I. Cisarova, Z. Padelkova and M. Budesinsky, *J. Org. Chem.*, 2010, **75**, 3443; (*e*) G. F. Wang, W. Zhang, Z. C. Lu, P. Wang, X. L. Zhang and Y. X. Li, *J. Org. Chem.*, 2009, **74**, 2508; (*f*) H. Dong, Z. Pei and O. Ramström, *Chem. Commun.*, 2008, 1359; (*g*) H. Dong, M. Rahm, T. Brinck and O. Ramström, *J. Am. Chem. Soc.*, 2008, **130**, 15270.

9 (*a*) B. Kalita, N. C. Barua, M. S. Bezbarua and G. Bez, *Synlett*, 2001, 1411; (*b*) G. Hasnaoui, J. H. L. Spelberg, E. de Vries, L. Tang, B. Hauer and D. B. Janssen, *Tetrahedron: Asymmetry*, 2005, **16**, 1685.

10 (*a*) S. Oae, N. Asai and K. Fujimore, *J. Chem. Soc., Perkin Trans. 2*, 1978, 571; (*b*) E. Iglesias, *J. Am. Chem. Soc.*, 1998, **120**, 13057.

11 F. Buckell, J. D. Hartry, U. Rajalingam, B. M. Bennett, R. A. Whitney and G. R. J. Thatcher, *J. Chem. Soc., Perkin Trans. 2*, 1994, 401.

12 Y. Zhao and D. G. Truhlar, *Theor. Chem. Acc.*, 2008, **120**, 215.

13 M. J. Frisch, *et al.*, *Gaussian 09, Revision A.1*, Gaussian, Inc., Wallingford, CT, 2009.

14 (*a*) Y. Zhao and D. G. Truhlar, *J. Chem. Theory Comput.*, 2011, **7**, 669; (*b*) R. Valero, J. R. B. Gomes, D. G. Truhlar and F. Illas, *J. Chem. Phys.*, 2008, **129**, 124710.

15 S. Sinnecker, A. Rajendran, A. Klamt, M. Diedenhofen and F. Neese, *J. Phys. Chem. A*, 2006, **110**, 2235.

16 S. Grimme, *J. Chem. Phys.*, 2003, **118**, 9095.